Supporting Information for

Construction of fluorescent screening system of allosteric modulators for $GABA_A$ receptor using turn-on probe

Seiji Sakamoto,[1] Kei Yamaura,[1,†] Tomohiro Numata,[2] Fumio Harada,[1] Kazuma Amaike,[1] Ryuji Inoue,[2] Shigeki Kiyonaka,[1,††] and Itaru Hamachi*[1,3]

[1] Department of Synthetic Chemistry and Biological Chemistry, Graduate School of Engineering, Kyoto University, Katsura, Nishikyo-ku, Kyoto 615-8510, Japan

[2] Department of Physiology, School of Medicine, Fukuoka University, 7-45-1 Nanakuma, Jonan-ku, Fukuoka 814-0180, Japan

[3] ERATO Innovative Molecular Technology for Neuroscience Project, Japan Science and Technology Agency (JST), Kyoto 615-8530, Japan

[†] Present address: Department of Molecular Imaging and Theranostics, National Institute of Radiological Sciences, QST, Anagawa 4-9-1, Inage-ku, Chiba 263-8555, Japan.

[††]Present address: Department of Biomolecular Engineering, Graduate School of Engineering, Nagoya University, Furo-cho, Chikusa-ku, Nagoya 464-8603, Japan

Correspondence: ihamachi@sbchem.kyoto-u.ac.jp (I.H.)

Table of Contents

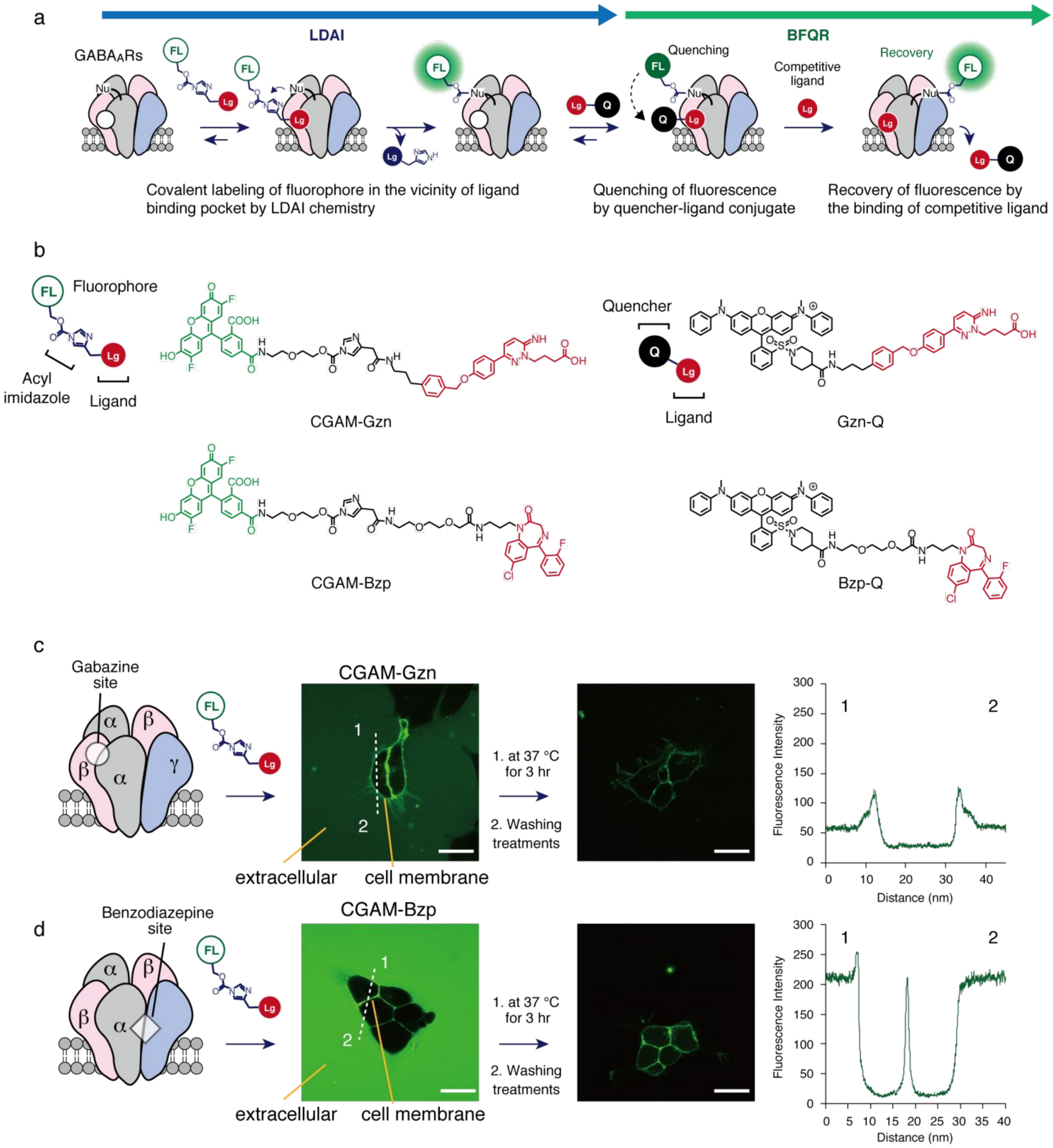

Figure S1. Chemical labeling of $GABA_A$Rs in HEK293T cells using CGAM reagents. (a) Schematic illustration of the construction of $GABA_A$R-based semisynthetic biosensors by a combination of LDAI with a BFQR method. (b) Structures of CGAM-Gzn, Gzn-Q, CGAM-Bzp, and Bzp-Q. (c,d) Representative confocal images of $GABA_A$R(α1/β3/γ2) transfected HEK293T cells labeled with CGAM-Gzn (1 μM) in c and CGAM-Bzp (1 μM) in d. The fluorescence intensity of OG fluorophore immediately after addition of labeling reagent in the dashed line was plotted. Scale bar = 20 μm.

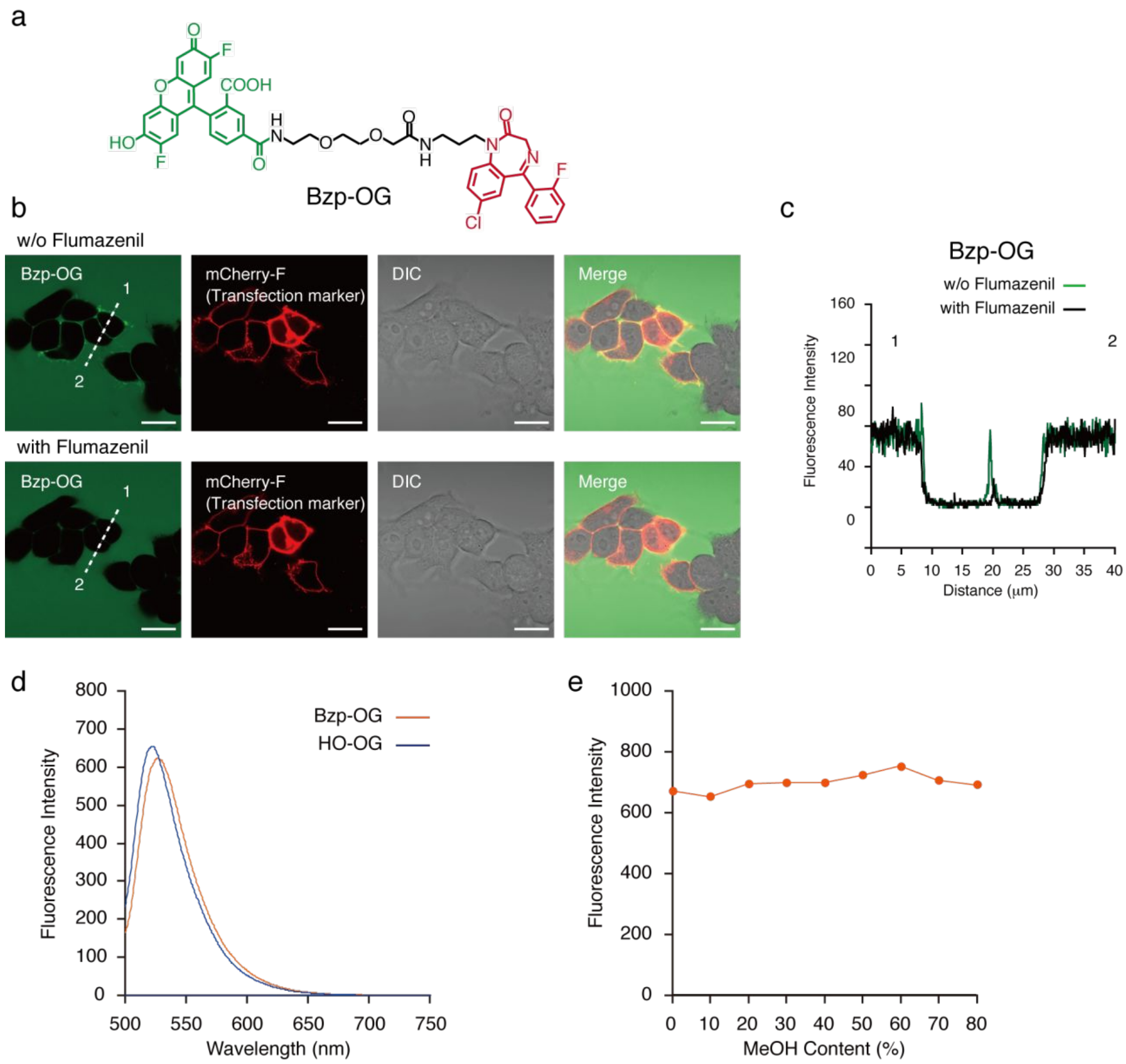

Figure S2. Characterization of an imaging probe, Bzp-OG. (a) Chemical structure of an imaging probe, Bzp-OG. (b) Confocal live cell imaging of HEK293T cells transfected with GABA$_A$R(α1/β3/γ2) upon addition of Bzp-OG (1 μM) in the presence or absence of gabazine (100 μM). Scale bar = 40 μm. (c) Fluorescence intensity analyses of the confocal images for Bzp-OG. The fluorescence intensity of OG fluorophore in the dashed line was plotted. (d) Fluorescence spectra of Bzp-OG (1 μM) or HO-OG (1 μM) in HBS buffer (pH 7.4) at r.t. λ_{ex} = 496 nm. (e) Plots of fluorescence intensities at peak tops with increasing MeOH content. See Figure S3d for these fluorescence spectra.

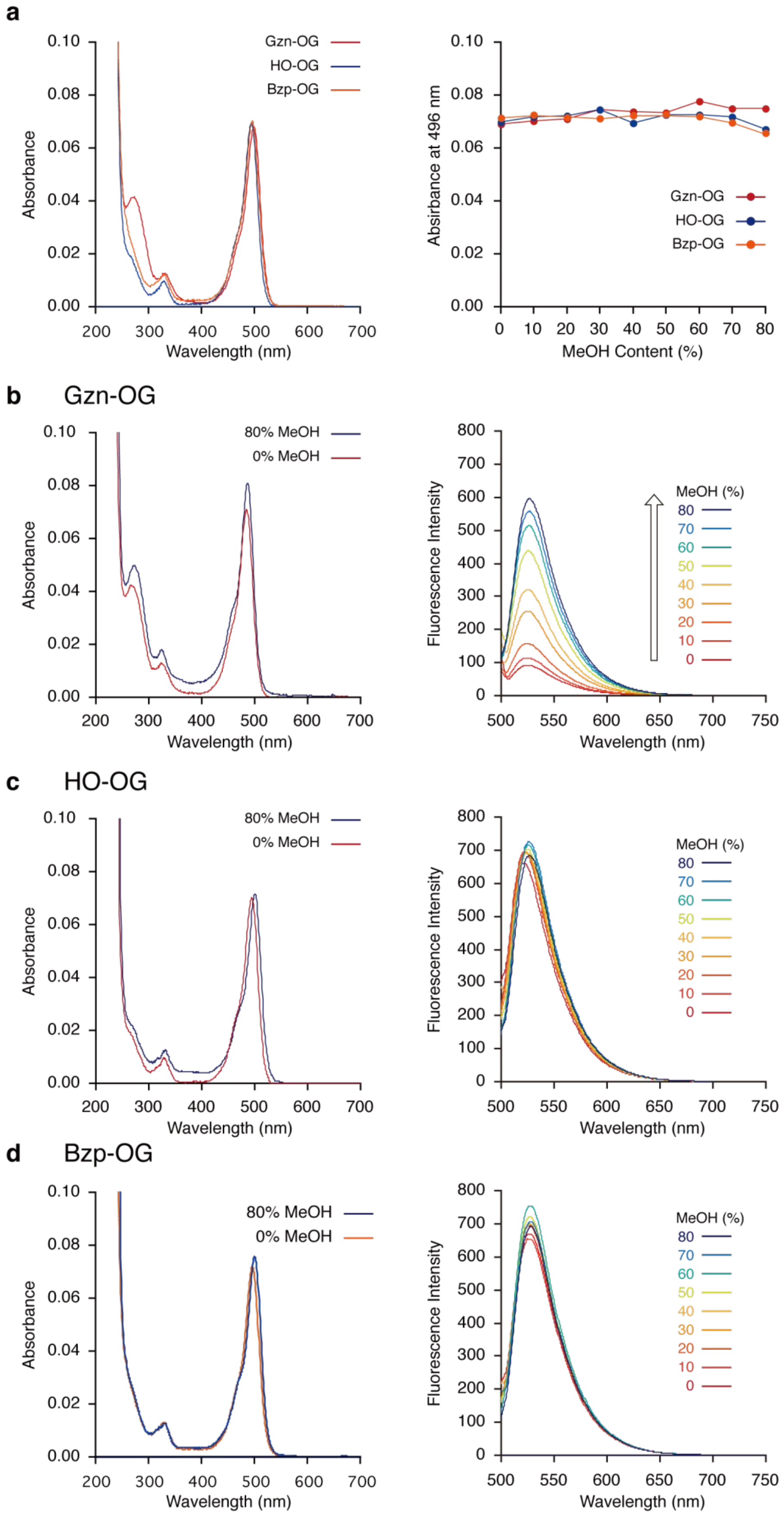

a
0.10
0.08
0.06
0.04
0.02
0.00
Absorbance
200 300 400 500 600 700
Wavelength (nm)
Gzn-OG
HO-OG
Bzp-OG
Absirbance at 496 nm
0 10 20 30 40 50 60 70 80
MeOH Content (%)
b Gzn-OG
80% MeOH
0% MeOH
Fluorescence Intensity
800 700 600 500 400 300 200 100 0
500 550 600 650 700 750
MeOH (%)
80 70 60 50 40 30 20 10 0
c HO-OG
d Bzp-OG

Figure S3. Photochemical properties of Gzn-OG, HO-OG, and Bzp-OG. (a) UV-Vis absorption spectra of compounds in HBS buffer (pH 7.4) at r.t. (left). Plots of absorbance at 496 nm with increasing MeOH content (right). (b) UV-Vis absorption spectra of Gzn-OG in the presence or absence of 80% MeOH at r.t. (left). The fluorescent spectral change of Gzn-OG with increasing MeOH content (right). [compound] = 1 μM and λ_{ex} = 496 nm. (c) UV-Vis absorption spectra of HO-OG in the presence or absence of 80% MeOH at r.t. (left). The fluorescent spectral change of HO-OG with increasing MeOH content (right). [compound] = 1 μM and λ_{ex} = 496 nm. (d) UV-Vis absorption spectra of Bzp-OG in the presence or absence of 80% MeOH at r.t. (left). The fluorescent spectral change of Bzp-OG with increasing MeOH content (right). [compound] = 1 μM and λ_{ex} = 496 nm.

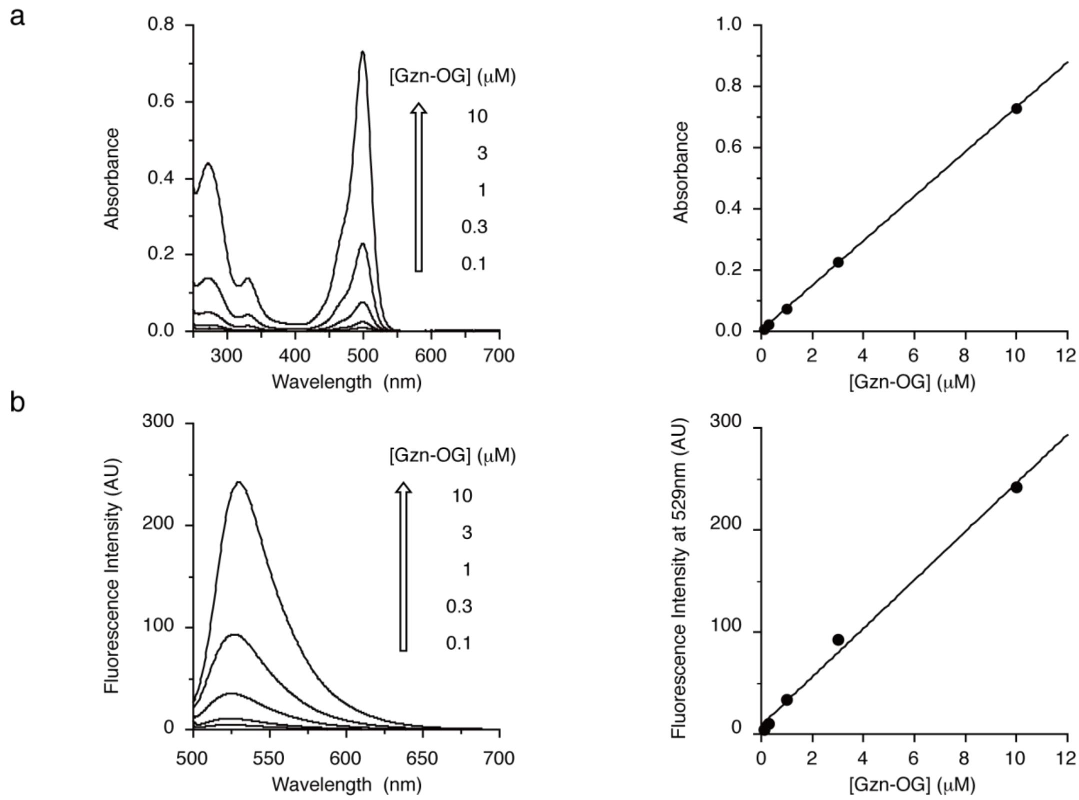

Figure S4. Concentration-dependency of Gzn-OG on UV-Vis and fluorescence spectra. (a) UV-Vis absorption spectra of Gzn-OG at different concentrations in HBS buffer (pH7.4) at r.t. (b) Fluorescence spectra of Gzn-OG at different concentrations in HBS buffer (pH7.4) at r.t. λ_{ex} = 496 nm.

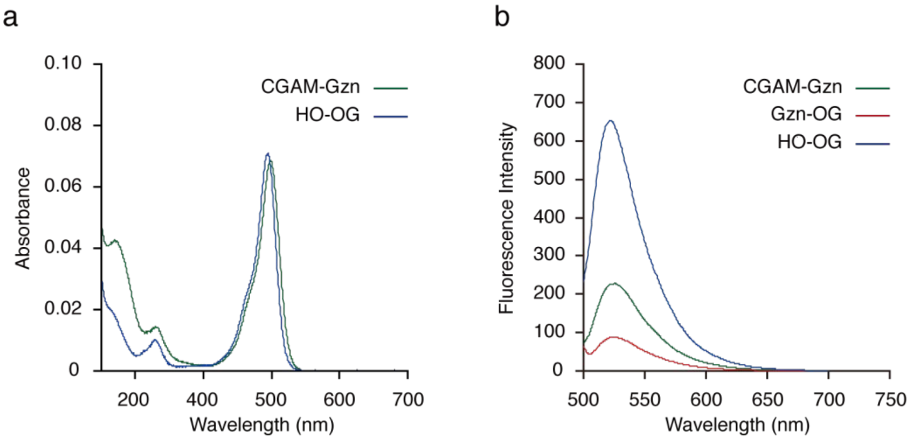

Figure S5. Photochemical properties of CGAM-Gzn. (a) UV-Vis absorption spectra of CGAM-Gzn and HO-OG in HBS buffer (pH 7.4) at r.t. The spectrum of HO-OG was shown for the comparison. [compound] = 1μM. (b) Fluorescence spectra of Gzn-OG, HO-OG, and CGAM-Gzn in HBS buffer (pH 7.4) at r.t. The fluorescence spectra of Gzn-OG and HO-OG were also shown for comparing the fluorescence intensity in the buffer. [compound] = 1 μM and λ_{ex} = 496 nm.

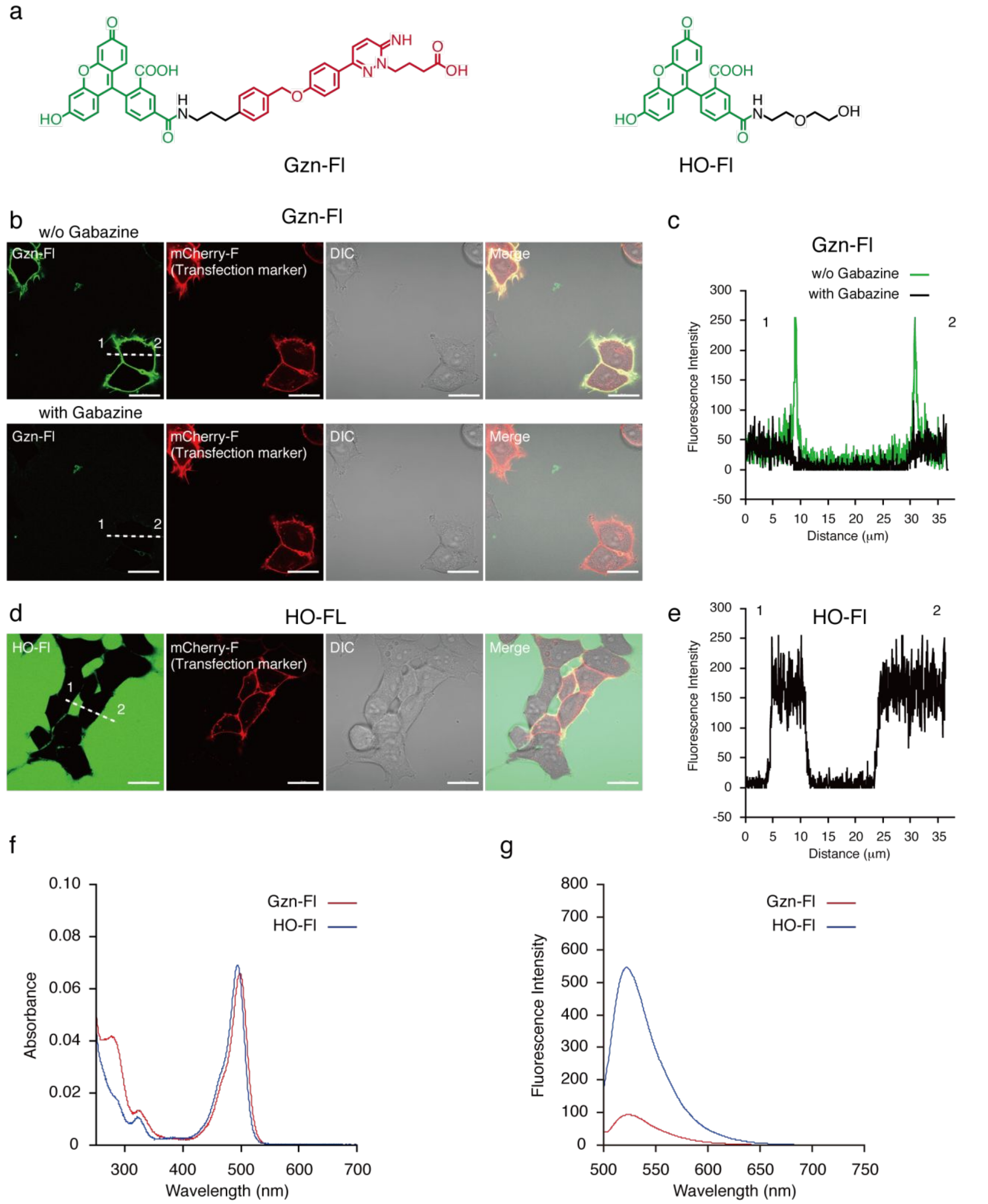

Figure S6. Characterization of a turn-on fluorescent imaging probe, Gzn-Fl. (a) Chemical structure of a turn-on fluorescent imaging probe, Gzn-Fl, and a control fluorophore, HO-Fl. (b and d) Confocal live cell imaging of HEK293T cells transfected with GABA$_A$R(α1/β3/γ2) upon addition of Gzn-Fl (1 μM) (b) or HO-Fl (1 μM) (d) in the presence or absence of gabazine (100 μM). Scale bar = 20 μm. (c and e) Fluorescence intensity analyses of the confocal images for Gzn-Fl (c) and HO-Fl (e). (f) UV-Vis absorption spectra of Gzn-Fl (1 μM) or HO-Fl (1 μM) in HBS buffer (pH 7.4) at r.t. (g) Fluorescence spectra of Gzn-Fl (1 μM) or HO-Fl (1 μM) in HBS buffer (pH 7.4) at r.t. λ_{ex} = 496 nm.

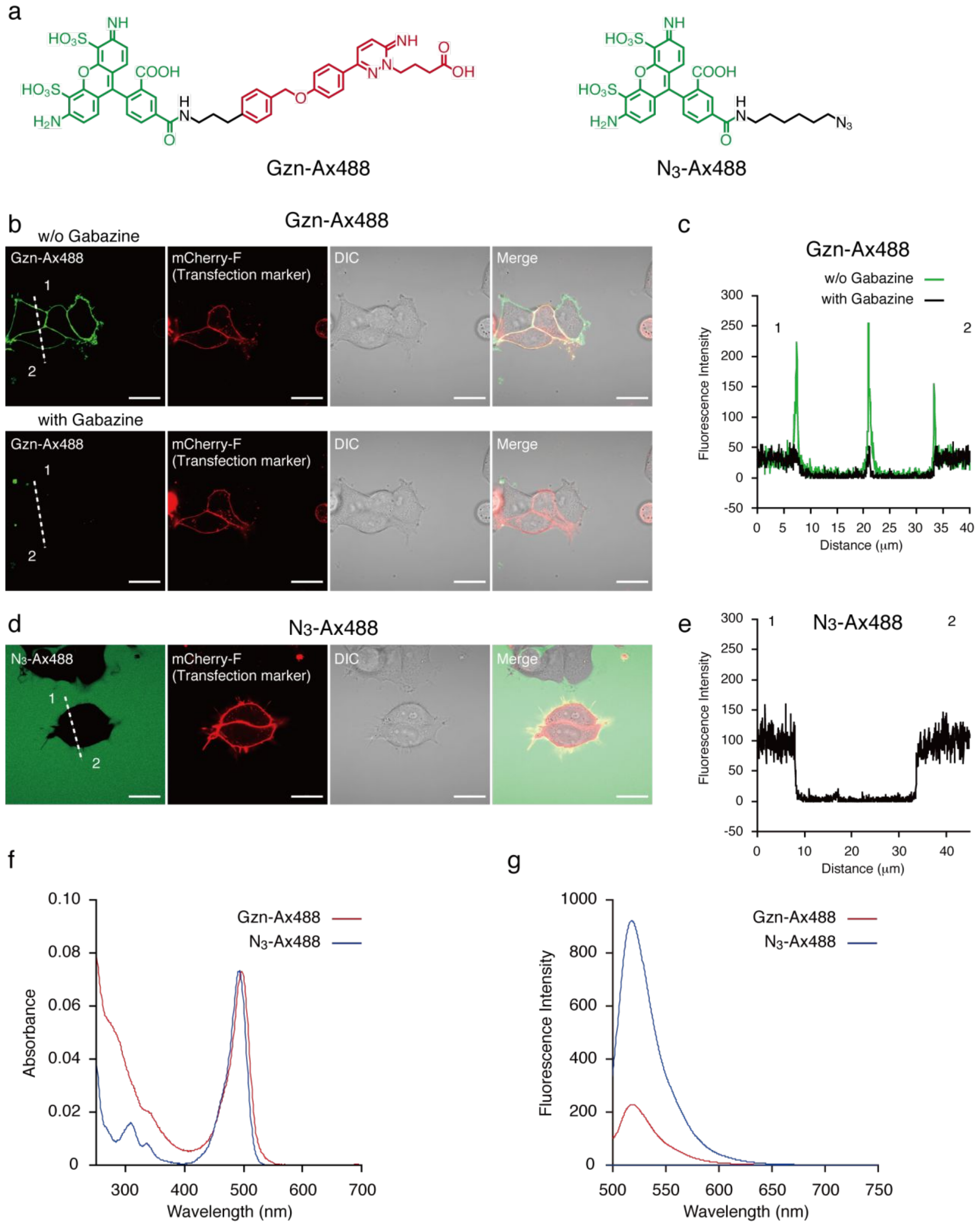

Figure S7. Characterization of a turn-on fluorescent imaging probe, Gzn-Ax488. (a) Chemical structure of a turn-on fluorescent imaging probe, Gzn-Ax488, and a control fluorophore, N_3-Ax488. (b and d) Confocal live cell imaging of HEK293T cells transfected with $GABA_AR(\alpha1/\beta3/\gamma2)$ upon addition of Gzn-Ax488 (1 μM) (b) or N_3-Ax488 (1 μM) (d) in the presence or absence of gabazine (100 μM). Scale bar = 20 μm. (c and e) Fluorescence intensity analyses of the confocal images for Gzn-Ax488 (c) and N_3-Ax488 (e). (f) UV-Vis absorption spectra of Gzn-Ax488 (1 μM) or N_3-Ax488 (1 μM) in HBS buffer (pH 7.4) at r.t. (g) Fluorescence spectra of Gzn-Ax488 (1 μM) or N_3-Ax488 (1 μM) in HBS buffer (pH 7.4) at r.t. λ_{ex} = 496 nm.

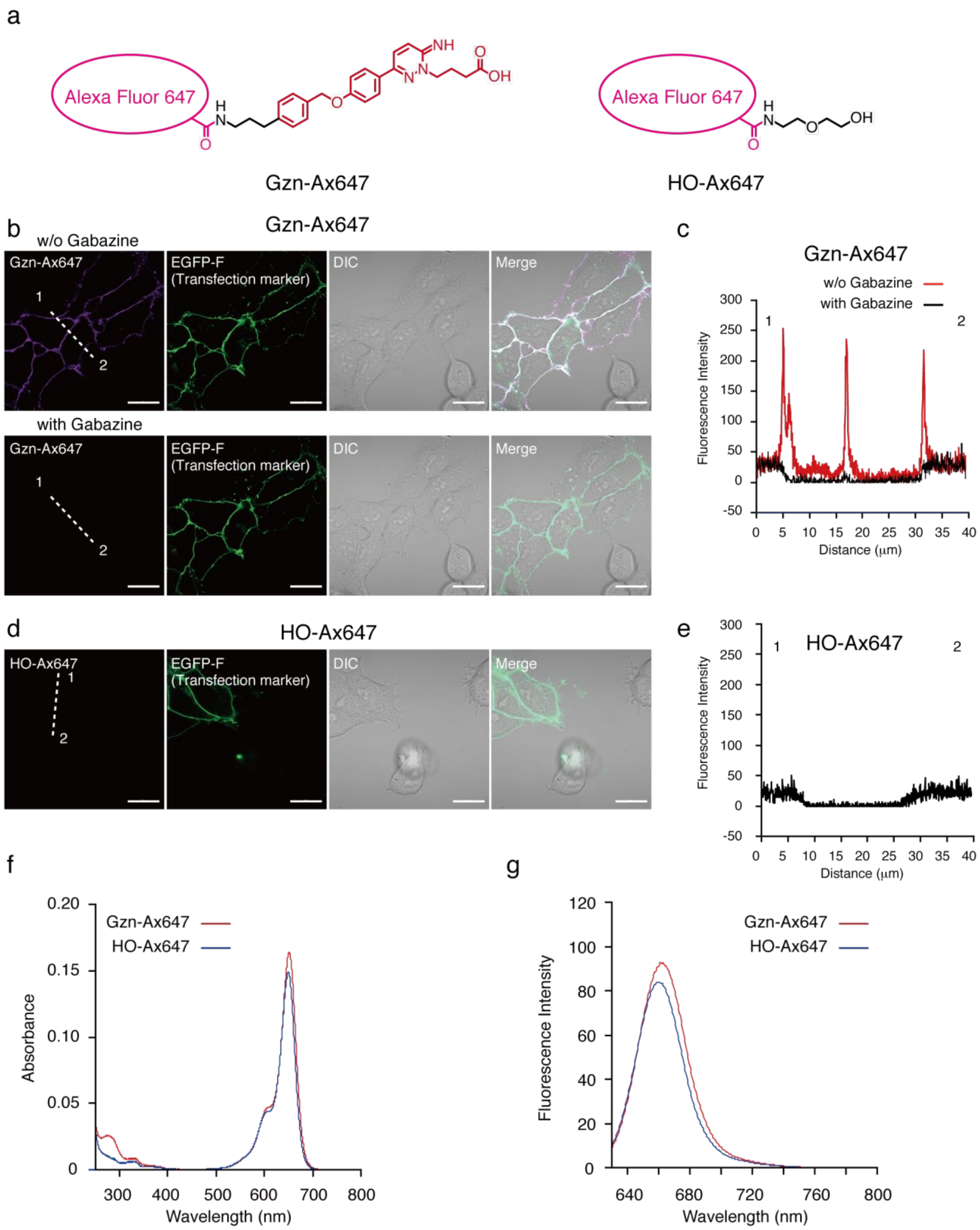

Figure S8. Characterization of a fluorescent imaging probe, Gzn-Ax647. (a) Chemical structure of an imaging probe, Gzn-Ax647, and a control fluorophore, HO-Ax647. (b and d) Confocal live cell imaging of HEK293T cells transfected with GABA$_A$R(α1/β3/γ2) upon addition of Gzn-Ax647 (1 μM) (b) or HO-Ax647 (1 μM) (d) in the presence or absence of gabazine (100 μM). Scale bar = 20 μm. (c and e) Fluorescence intensity analyses of the confocal images for Gzn-Ax647 (c) and HO-Ax647 (e). (f) UV-Vis absorption spectra of Gzn-Ax647 (0.5 μM) or HO-Ax647 (0.5 μM) in HBS buffer (pH 7.4) at r.t. (g) Fluorescence spectra of Gzn-Ax647 (0.5 μM) or HO-Ax647 (0.5 μM) in HBS buffer (pH 7.4) at r.t. λ_{ex} = 650 nm.

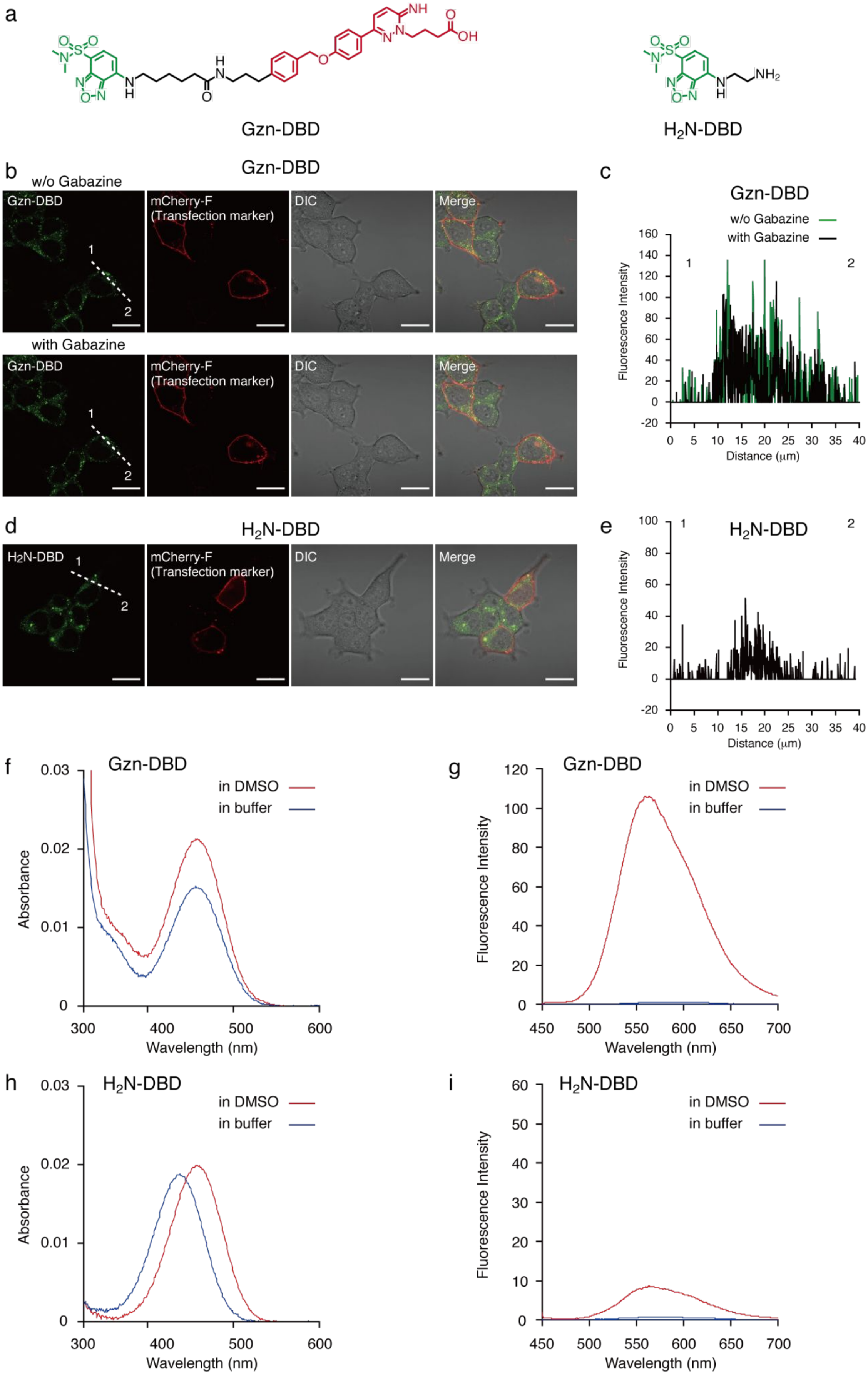
a
Gzn-DBD
H2N-DBD
b
Gzn-DBD
w/o Gabazine
with Gabazine
mCherry-F
(Transfection marker)
DIC
Merge
c
Fluorescence Intensity
Distance (μm)
d
e
f
g
h
i
in DMSO
in buffer
Absorbance
Wavelength (nm)

Figure S9. Characterization of a fluorescent imaging probe, Gzn-DBD. (a) Chemical structure of a turn-on fluorescent imaging probe, Gzn-DBD, and a control fluorophore, H_2N-DBD. (b and d) Confocal live cell imaging of HEK293T cells transfected with $GABA_AR(\alpha1/\beta3/\gamma2)$ upon addition of Gzn-DBD (1 μM) or H_2N-DBD (1 μM) in the presence or absence of gabazine (100 μM). Scale bar = 20 μm. (c and e) Fluorescence intensity analyses of the confocal images for Gzn-DBD (c) and H_2N-DBD (e). (f and h) UV-Vis absorption spectra of Gzn-DBD (2 μM) (f) or H_2N-DBD (2 μM) (h) in DMSO or HBS buffer (pH 7.4) at r.t. (g and i) Fluorescence spectra of Gzn-DBD (2 μM) (f) or H_2N-DBD (2 μM) (i) in DMSO or HBS buffer (pH 7.4) at r.t. λ_{ex} = 430 nm.

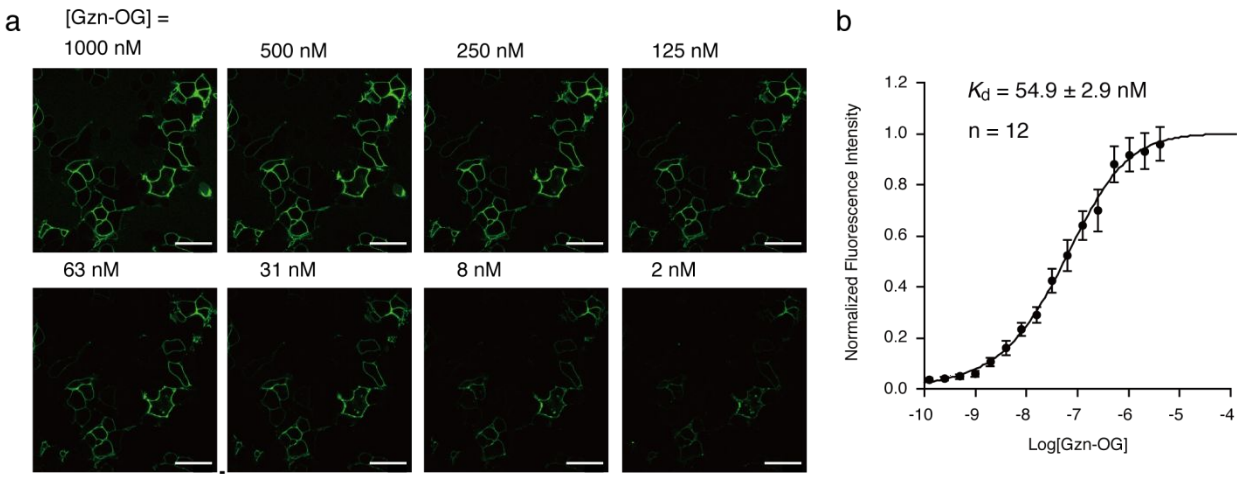

Figure S10. Determination of an affinity of Gzn-OG for $GABA_AR$s in HEK293T cells. (a) Confocal images of $GABA_AR$(α1/β3/γ2) transfected HEK293T cells at each concentration of Gzn-OG. Scale bar = 40 µm. (b) Plot of fluorescence intensity change of plasma membranes of cells. The dissociation constant of Gzn-OG for $GABA_AR$(α1/β3/γ2) was determined to be 54.9 nM by fitting the fluorescence intensity change with a theoretical logistic equation. Data represent mean ± SEM. n = 12.

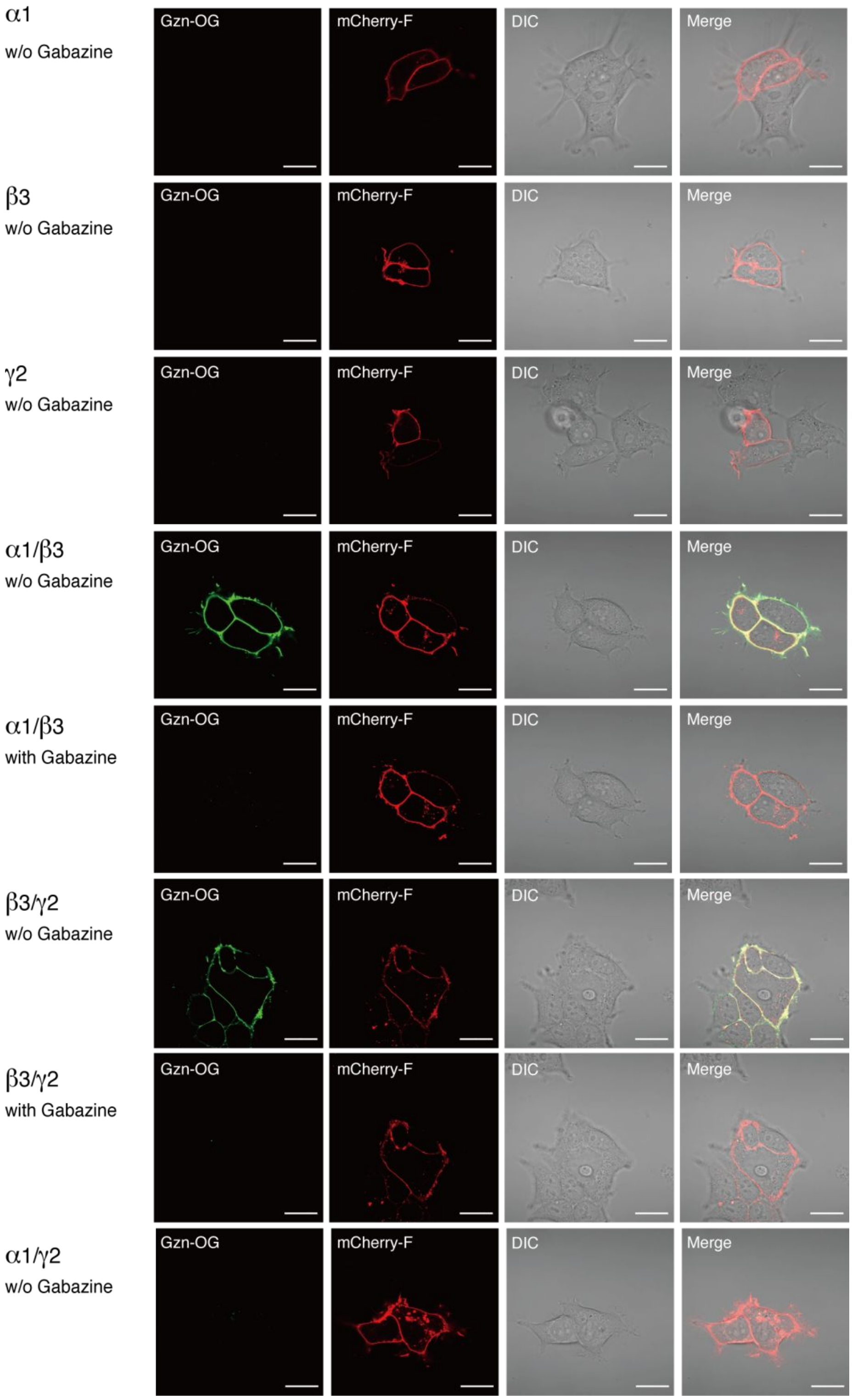

Figure S11. Subunit specificity for CLSM imaging of $GABA_AR$ using Gzn-OG. HEK293T cells transfected with varied compositions of the $GABA_AR$ subunits (a single subunit of α1, β3, or γ2; two subunits of α1/β3, α1/γ2 or β3/γ2) were treated with 100 nM Gzn-OG. Scale bar = 20 μm.

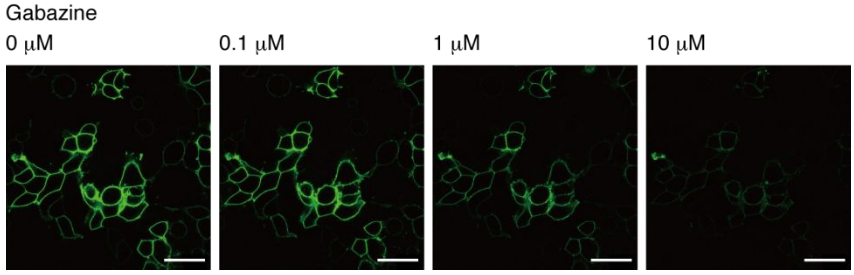

Figure S12. Confocal live cell imaging of HEK293T cells transfected with $GABA_AR(\alpha1/\beta3/\gamma2)$ upon addition of Gzn-OG (100 nM) at various concentrations of gabazine. Scale bar = 40 μm.

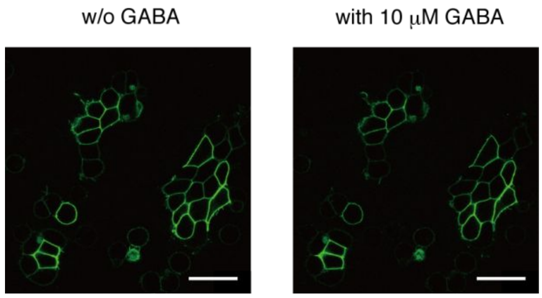

Figure S13. Confocal live cell imaging of HEK293T cells transfected with $GABA_AR(\alpha 1/\beta 3/\gamma 2)$ upon addition of Gzn-OG (100 nM) in the presence or absence of 10 μM GABA. Scale bar = 40 μm.

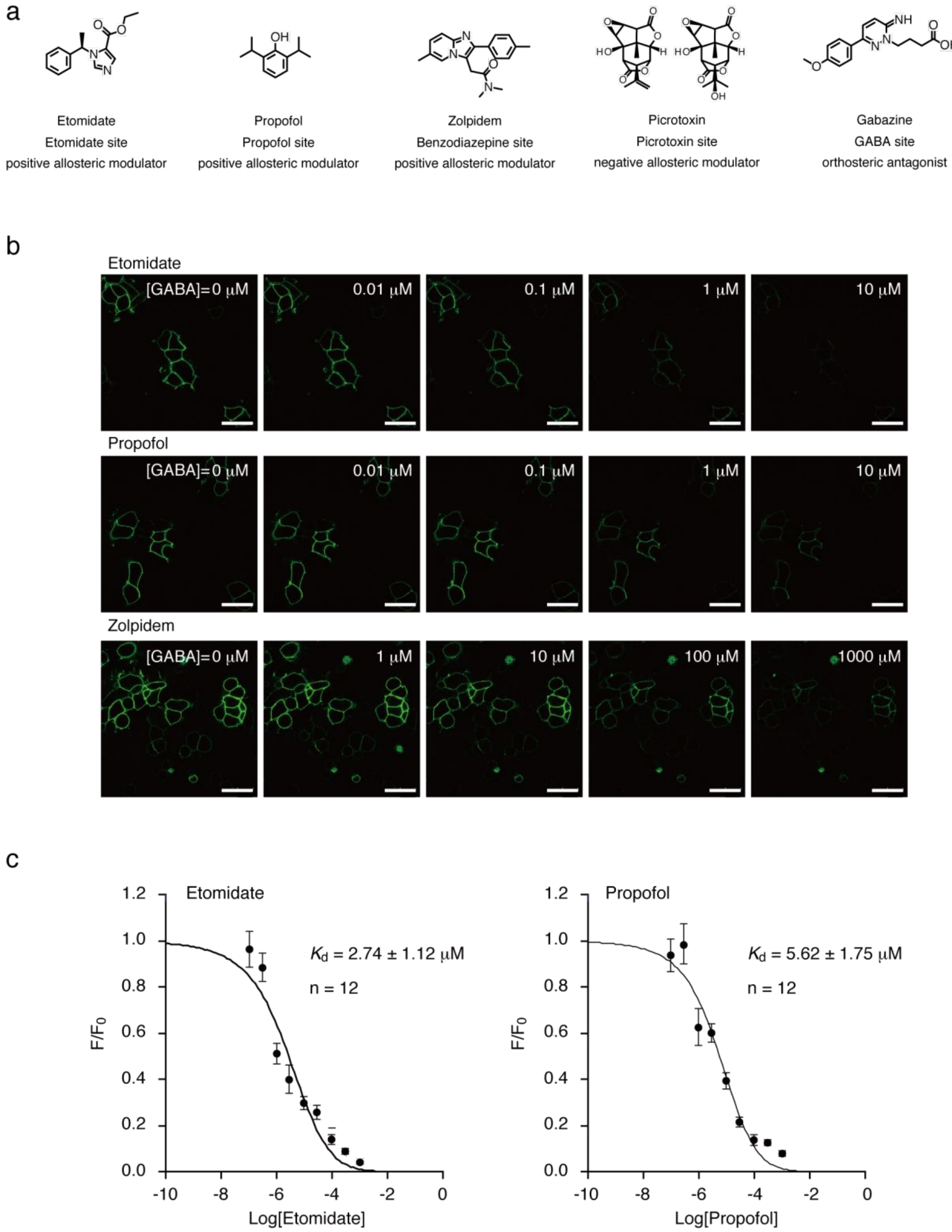

Figure S14. Binding assay of $GABA_A$R ligands using Gzn-OG in $GABA_A$R (α1/β3/γ2)-expressing HEK293T cells. (a) Chemical structure of representative positive allosteric modulators, a negative allosteric modulator, and an orthosteric ligand for $GABA_A$Rs used in this study. (b) Confocal live cell images of $GABA_A$R(α1/β3/γ2) expressing HEK293T cells upon addition of Gzn-OG (100 nM) and a PAM at various concentrations of GABA. The concentrations of Gzn-OG and a PAM were fixed in this assay. [etomidate] = 200 μM, [propofol] = 200 μM, and [zolpidem] = 20 μM. Scale bar = 40 μm. (c) Plots of fluorescence intensity (F/F_0) of plasma membranes of cells with increasing the PAM concentration in the presence of 10 μM GABA. The dissociation constants of etomidate and propofol for $GABA_A$R(α1/β3/γ2) were determined by fitting the fluorescence intensity change with a theoretical logistic equation. [Gzn-OG] = 100 nM. Data represent mean ± SEM. n = 12.

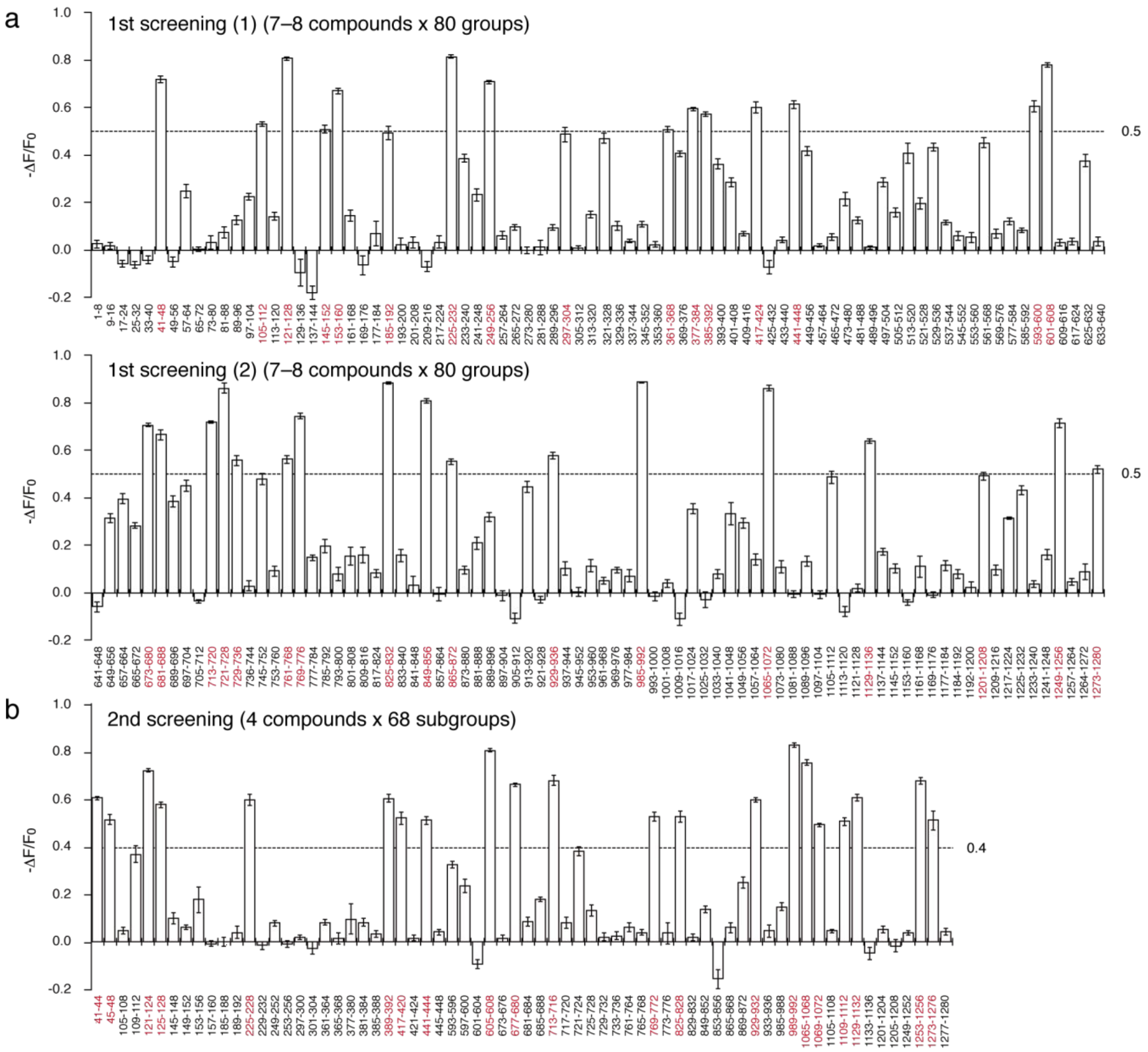

Figure S15. High-throughput screening of PAMs for GABA$_A$R(α1/β3/γ2) by a ligand assay system using Gzn-OG. (a) $-\Delta F/F_0$ values in the first screening process. The ligand assay system was treated with the mixture including 7 or 8 chemicals (the compounds exhibiting their intrinsic fluorescence were excluded in this assay). The final concentration of each compound was 10 μM. Threshold ($-\Delta F/F_0 = 0.5$) in this screening is shown as a dashed line. Data represent mean ± SEM. n = 7–12. The entire list of 1280 compounds can be found in Table S1. Hit groups are marked in red. (b) $-\Delta F/F_0$ values in the second screening process. The hit groups in the first screening were divided into two subgroups, and the ligand assay system was treated with each mixture including 4 chemicals. The final concentration of each compound was 10 μM. Threshold ($-\Delta F/F_0 = 0.4$) in this screening is shown as a dashed line. Data represent mean ± SEM. n = 8–12. Hit subgroups are marked in red.

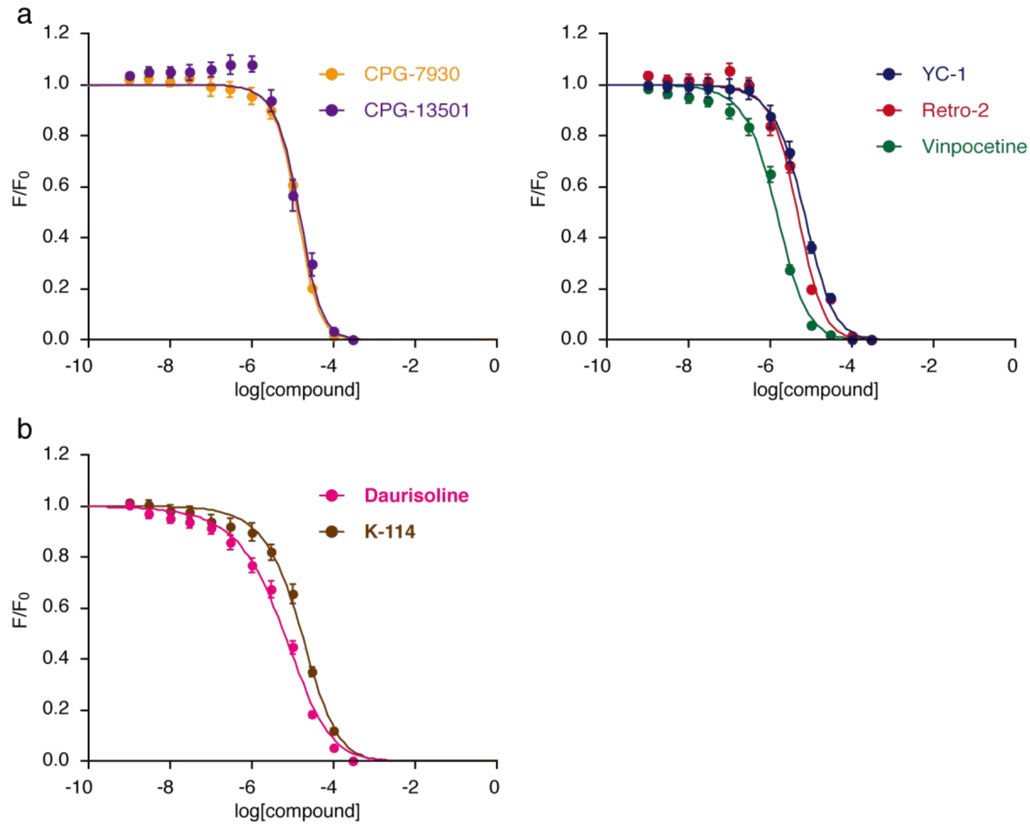

Figure S16. Characterization of hit compounds using Gzn-OG in $GABA_AR$ ($\alpha 1/\beta 3/\gamma 2$)-expressing HEK293T cells. (a) Plots of fluorescence intensity (F/F_0) of plasma membranes of cells with increasing each hit compound concentration in the presence of 10 μM GABA. The dissociation constants of hit compounds for $GABA_AR(\alpha 1/\beta 3/\gamma 2)$ were determined by fitting the fluorescence intensity change with a theoretical logistic equation (K_d = 13.1, 14.4, 1.4, 4.7, and 6.8 μM for CGP-7930, CGP-13501, vinpocetine, Retro-2, and YC-1, respectively). [Gzn-OG] = 100 nM and [GABA] = 10 μM. Data represent mean ± SEM. n = 10–12. (b) Plots of fluorescence intensity (F/F_0) of plasma membranes of cells with increasing the daurisoline and K-114 concentration in the absence of GABA. The K_d values were determined to be 2.2 and 5.8 μM for daurisoline and K-114, respectively, by fitting the fluorescence intensity (F/F_0) with a theoretical logistic equation. [Gzn-OG] = 100 nM, Data represent mean ± SEM. n = 12.

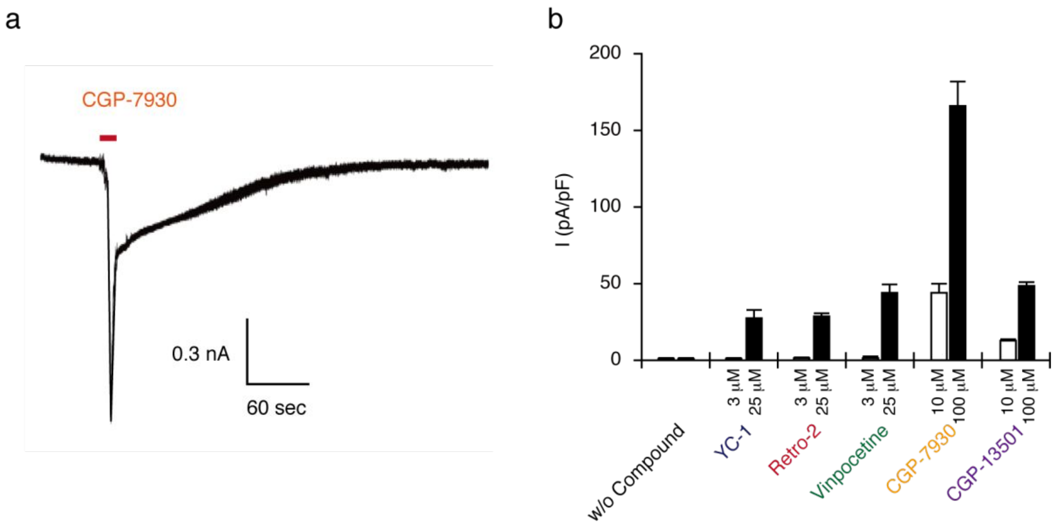

Figure S17. Electrophysiological characterization of hit compounds. (a) CGP-7930 induced whole cell currents without GABA. A representative time course of whole cell currents recorded at –60 mV in HEK293T cells transfected with $GABA_AR$(α1/β3/γ2) by the addition of CGP-7930. Red bar indicates the period of 100 μM CGP-7930. (b) Effects of YC-1, Retro-2, vinpocetine, CPG-7930, and CPG-13501 on the whole-cell currents in $GABA_AR$ (α1/β3/γ2)-expressing HEK293T cells at high (100 μM for CGP-7930 and CGP-13501, 25 μM for vinpocetine, Retro-2, and YC-1) and low (10 μM for CGP-7930 and CGP-13501, 3 μM for vinpocetine, Retro-2, and YC-1) concentrations.

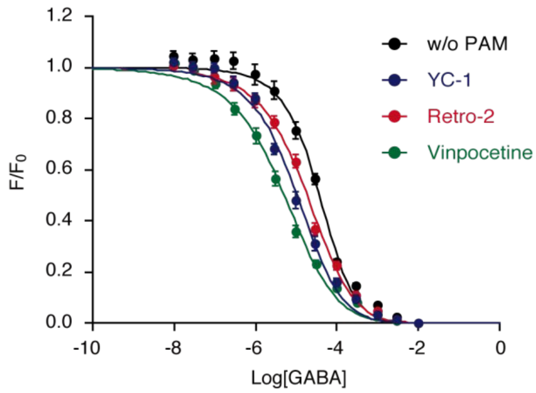

Figure S18. Plots of fluorescence intensity (F/F_0) of plasma membranes of cells with increasing GABA concentration in the presence or absence of a hit compound. HEK293T cells transfected with $GABA_A$R(α1/β3/γ2) were treated with 100 nM Gzn-OG and 3 μM of each hit compound, then fluorescence intensity of cells was measured by confocal microscopy with increasing GABA concentration. The concentrations of Gzn-OG and a hit compound were fixed in this assay. The K_d values of GABA in the presence of each hit compound were determined by fitting the fluorescence change with a logistic equation (1.8, 6.7, and 3.9 μM for vinpocetine, Retro-2, and YC-1, respectively). Data represent mean ± SEM. n = 12.

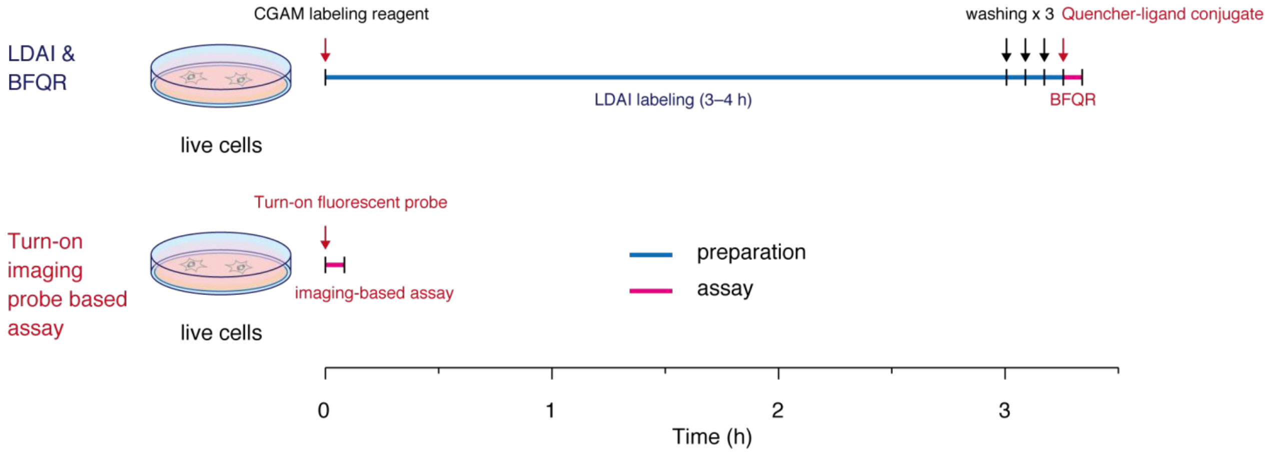

Figure S19. The flowcharts of experimental procedures for LDAI & BFQR-based fluorescent assay or present (turn-on imaging probe based) assay.

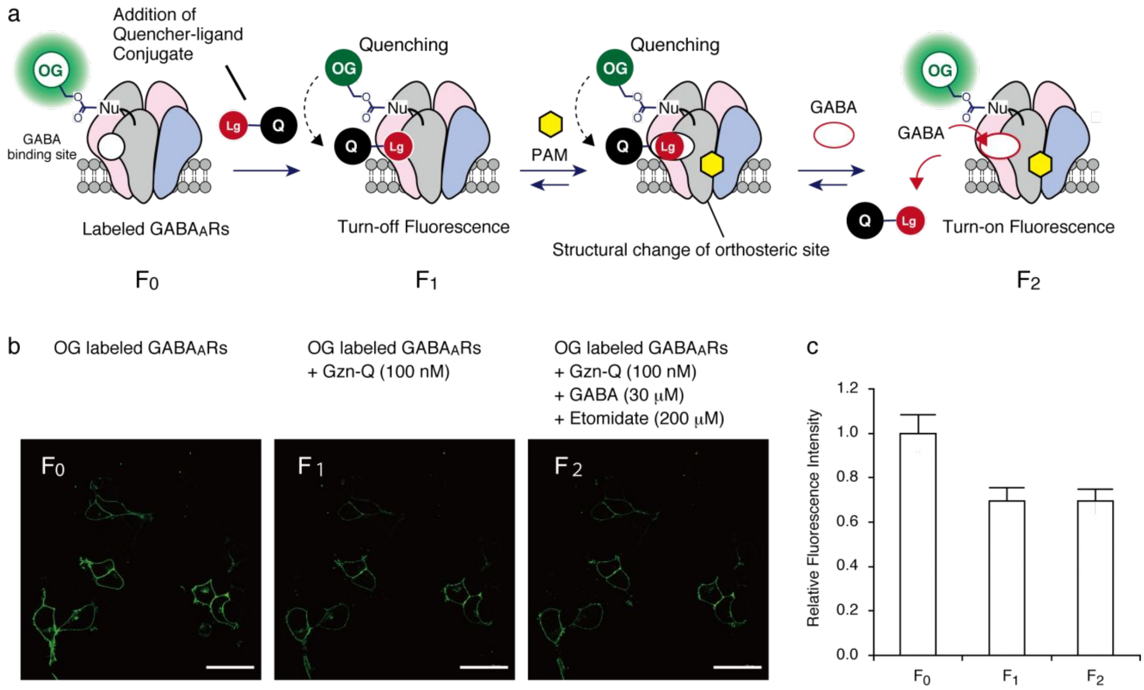

Figure S20. Construction of GABA$_A$R-based semisynthetic biosensors by a combination of LDAI with a BFQR method for sensing PAMs. (a) Schematic illustration of the assay system for detecting PAMs. (b) Representative confocal images of GABA$_A$R(α1/β3/γ2) transfected HEK293T cells labeled with CGAM-Gzn (1 μM) at 37 °C for 3 hr to obtain OG-labeled GABA$_A$R(α1/β3/γ2) (OG-GABA$_A$R(α1/β3/γ2)). The cells were treated with 100 nM Gzn-Q, and then GABA (30 μM) and etomidate (200 μM) were added into the cell cultured dish. Scale bar = 40 μm. (c) Normalized fluorescence intensity of OG-GABA$_A$R(α1/β3/γ2) (F_0), the quenched fluorescence by Gzn-Q (F_1), and the fluorescence after addition of GABA (30 μM) and etomidate (200 μM) (F_2). The fluorescence intensity was obtained from CLSM images. Data represent mean ± SEM. n = 8.

Supporting Notes

Synthesis and Characterization

General materials and methods for organic synthesis

All chemical reagents and solvents were obtained from commercial suppliers (Aldrich, Tokyo Chemical Industry (TCI), Wako Pure Chemical Industries, Acros Organics, Sasaki Chemical, or Watanabe Chemical Industries) and used without further purification. Thin layer chromatography (TLC) was performed on silica gel 60 F_{254} precoated aluminum sheets (Merck) and visualized by fluorescence quenching or ninhydrin staining. Chromatographic purification was conducted by flash column chromatography on silica gel 60N (neutral, 40–50 μm, Kanto Chemical). ^{1}H-NMR spectra were recorded in deuterated solvents on a Varian Mercury 400 (400 MHz). Chemical shifts were referenced to residual solvent peaks or tetramethylsilane (δ = 0 ppm). Multiplicities are abbreviated as follows: s = singlet, d = doublet, t = triplet, m = multiplet. MALDI-TOF Mass spectra were measured on Autoflex II (Bruker Daltonics). High resolution mass spectra were measured on an Exactive (Thermo Scientific) equipped with electron spray ionization (ESI). Reversed-phase HPLC (RP-HPLC) was carried out on a Hitachi Chromaster system equipped with a diode array and a YMC-Pack ODS-A column.

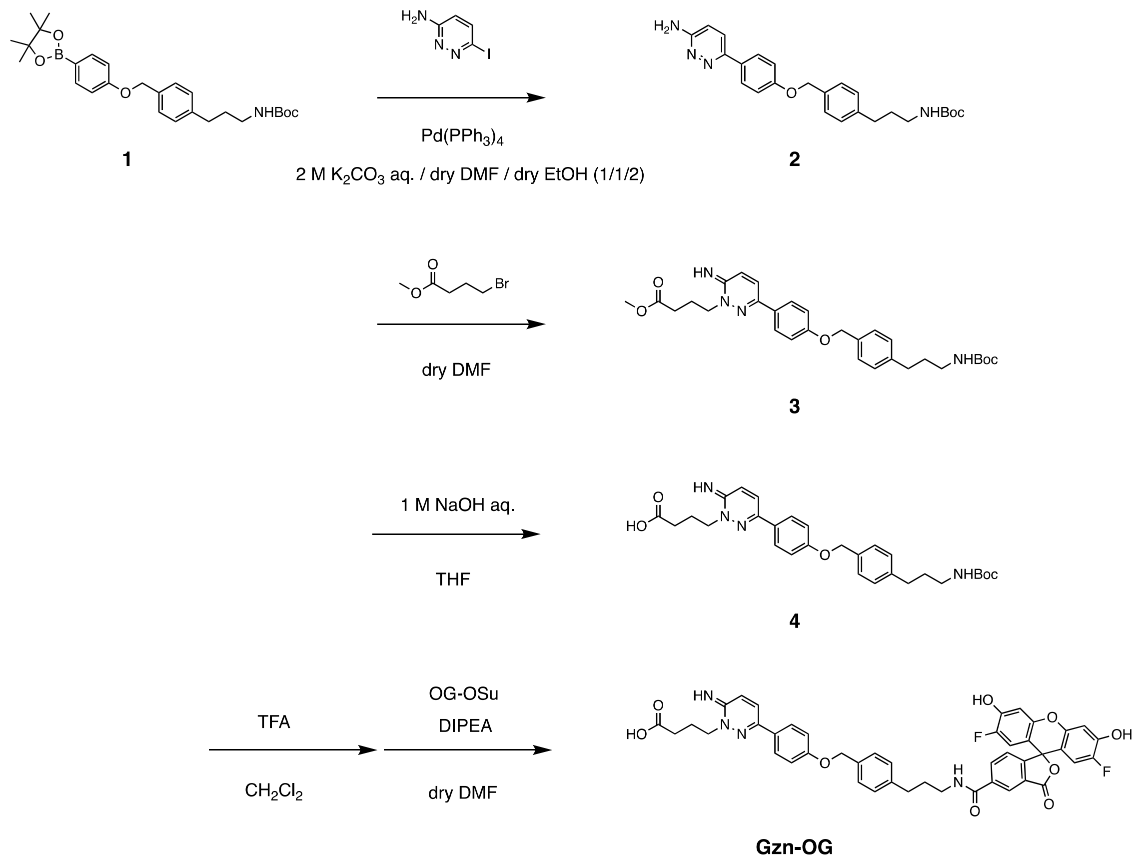

Synthesis of 2

***tert*-butyl (3-(4-((4-(6-aminopyridazin-3-yl)phenoxy)methyl)phenyl)propyl)carbamate (4)**

Compound **1** (83 mg, 0.18 mmol)[S1], 6-iodopyridazin-3-amine (53 mg, 0.24 mmol), Pd $(PPh_3)_4$ (12 mg, 10 μmol) were dissolved in 2 M Na_2CO_3 : dry DMF : dry EtOH = 1 : 1 : 2 (8 mL) under N_2 atmosphere. The reaction mixture was allowed to stir for 2.5 h at 95 °C. The solution was diluted with $CHCl_3$ (30 mL) and washed with H_2O (30 mL x 4). The organic layer was dried over Na_2SO_4, filtered, evaporated. The residue was purified by silica gel column chromatography ($CHCl_3$: MeOH = 20:1) to yield compound **2** (77 mg, 0.17 mmol, 94%) as a white solid. ^{1}H-NMR (400 MHz, $CDCl_3$): δ 7.89 (d, 2H, *J* = 8.4 Hz), 7.57 (d, 1H, *J* = 9.2 Hz), 7.36 (d, 2H, *J* = 8.0 Hz), 7.20 (d, 2H, *J* = 7.6 Hz), 7.05 (d, 2H, *J* = 8.8 Hz), 6.80 (d, 1H, *J* = 9.2 Hz), 5.07 (s, 2H), 4.77 (s, 2H), 4,56 (broad d, 1H), 3.16 (m, 2H), 2.65 (d, 2H, *J* = 8.0 Hz), 1.81 (tm 2H), 1.44 (s, 9H).

Synthesis of 3

Methyl 4-(3-(4-((4-(3-((*tert*-butoxycarbonyl)amino)propyl)benzyl)oxy)phenyl)-6-iminopyridazin-1(6H)-yl)butanoate (3)

To a stirred solution of compound **2** (38 mg, 87 μmol) in dry DMF (0.29 mL) was added methyl 4-bromobutanoate (17 mg, 94μmol, 1.1 eq) under N_2 atmosphere. The reaction mixture was allowed to stir for 2 h at 80 °C. The solution was diluted with $CHCl_3$: MeOH = 10:1 (1 mL) and washed with an alkaline brine (pH = 14) (1 mL x 1). The organic layer was dried over Na_2SO_4, filtered, evaporated. The residue was purified by silica gel column chromatography ($CHCl_3$: MeOH = 10:1 containing 1% NH_3 aq.) to yield compound **3** (16 mg, 28 μmol, 32%) as a white solid. ^{1}H-NMR (400 MHz, CD_3OD): δ 7.80 (d, 2H, *J* = 9.2 Hz), 7.63 (d, 1H, *J* = 10.0 Hz), 7.38 (d, 2H, *J* = 7.6 Hz), 7.25 (d, 2H, *J* = 8.0 Hz), 7.15 (d, 2H, *J* = 9.6 Hz), 7.09 (d, 2H, *J* = 8.8 Hz), 5.12 (s, 2H), 4.22 (t, 2H, *J* = 6.8 Hz), 3.63 (s, 3H), 3.08 (m, 2H), 2.66 (t, 2H, *J* = 7.8 Hz), 2.52 (t, 2H, *J* = 7.0 Hz), 2.19 (m, 2H), 1.80 (m, 2H), 1.47 (s, 9H).

Synthesis of Gzn-OG

4-(3-(4-((4-(3-(2',7'-difluoro-6'-hydroxy-3'-oxo-3',9a'-dihydro-3H-spiro[isobenzofuran-1,9'-xanthene]-5-carboxamido)propyl)benzyl)oxy)phenyl)-6-iminopyridazin-1(6H)-yl)butanoic acid (Gzn-OG)

To a stirred solution of compound **3** (9 mg, 17 μmol) in THF (100 μL) and H_2O (30 μL) was added 1 M NaOH (70 μL). The reaction mixture was allowed to stir for 30 min at r.t. The solution was neutralised with 1 M HCl. The solution was evaporated to give **4** as a white solid. The crude product was dissolved in CH_2Cl_2 (1 mL) and TFA (1 mL), and the reaction mixture was allowed to stir for 1.5 h at r.t. After azetoropic removal of TFA with toluene (2 mL x 2), the residue was dissolved in dry DMF (170 µL). Then, Oregon Green succinimide ester (OG-OSu) (6.4 mg, 13 µmol, 0.8 eq.) and DIPEA (7.7 mg, 56 µmol, 4.6 eq.) were added. The reaction mixture was stirred at r.t. for 3 h. The solution was purified by HPLC to yield compound Gzn-OG (6 mg, 6.5 µmol, 41%) as an orange solid. ^{1}H-NMR (400 MHz, CD_3OD): δ 8.41 (s, 1H), 8.29 (d, 1H, J = 9.6 Hz), 8.15 (d, 1H, J = 8.0 Hz), 7.95 (d, 2H, J = 8.4 Hz), 7.61 (d, 1H, J = 9.6 Hz), 7.41 (d, 2H, J = 8.0 Hz), 7.35 (d, 1H, J = 8.4 Hz), 7.32 (d, 2H, J = 8.0 Hz), 7.14 (d, 2H, J = 8.4 Hz), 6.88 (s, 1H), 6.86 (s, 1H), 6.48 (s, 1H), 6.45 (s, 1H), 5.15 (s, 2H), 4.46 (t, 2H, J = 7.2 Hz), 3.50 (m, 2H), 2.80 (t, 2H, J = 7.6 Hz), 2.59 (t, 2H, J = 6.6 Hz), 2.26 (m, 2H), 2.02 (m, 2H). ^{13}C-NMR-dept (500 MHz, CD_3OD): δ 176.40, 168.40, 162.76, 153.90, 152.09, 143.14,138.46, 135.74, 132.61, 129.73, 129.32, 128.92, 126.65, 126.52, 116.65, 114.47, 114.30, 106.19, 71.12, 56.84, 41.07, 34.21, 31.84, 30.73, 22.69. HR-ESI MS: calcd for $C_{45}H_{37}F_2N_4O_9$ $[M+H]^+$ = 815.2523: obsd = 815.2523.

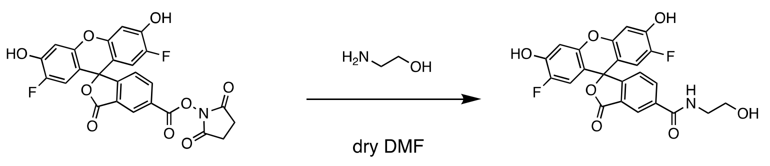

Synthesis of HO-OG

2',7'-difluoro-3',6'-dihydroxy-N-(2-hydroxymethyl)-3-oxo-3H-spiro[isobenzofuran-1,9'-xanthene]-5-carboxyamide

OG-OSu (2 mg, 3.9 µmol) was dissolved into 0.2 mL of super dehydrated DMF. 2-Aminoethanol (5 µL, 83 µmol, 21 equiv.) was added and the reaction solution was stirred at r.t. under Ar atmosphere for 1 h. The reaction was stopped by adding 1.5 mL of 66 % MeCN / water containing 0.1% TFA. The HO-OG was purified with reversed-phase HPLC and lyophilized (orange solid, 1.4 mg, 78%). ^{1}H-NMR (400 MHz, CD_3OD): δ 8.50 (s, 2H), 8.24 (d, 7.35 (d, 1H, J = 7.9 Hz), 6.85 (d, 2H, J = 7.4 Hz), 6.50 (d, 2H, J = 11.0 Hz), 3.76 (t, 2H, J = 6.1 Hz), 3.57 (t, 2H, J = 5.8 Hz). ^{13}C-NMR-dept (500 MHz, DMF-d7): δ 168.54, 166.17, 153.06, 150.65, 149.38, 149.05, 138.02, 134.78, 128.39, 125.47, 125.04, 114.04, 109.64, 105.91, 61.29, 43.71. HR-ESI MS: calcd for $C_{23}H_{16}F_2NO_7$ $[M+H]^+$ = 454.0744: obsd = 454.0745.

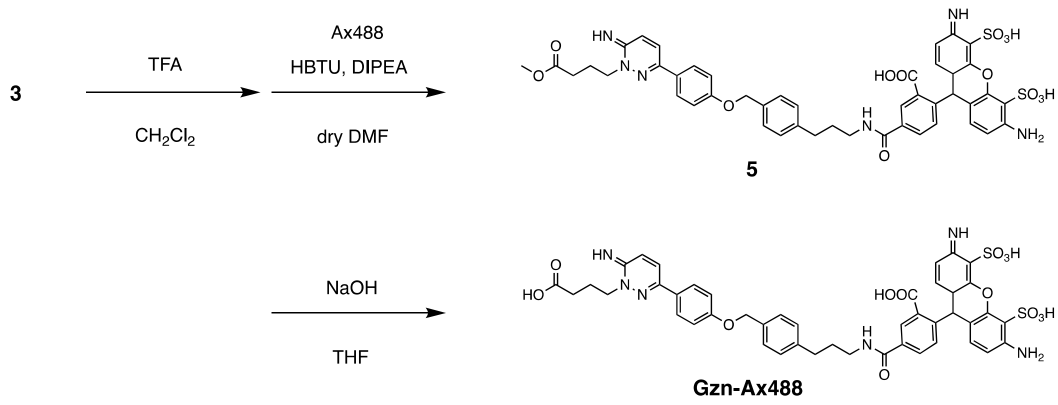

Synthesis of Gzn-Ax488

2-(6-amino-3-imino-4,5-disulfo-9,9a-dihydro-3*H*-xanthen-9-yl)-5-((3-(4-((4-(1-(3-carboxypropyl)-6-imino-1,6-dihydropyridazin-3-yl)phenoxy)methyl)phenyl)propyl)carbamoyl)benzoic acid

To a stirred solution of compound **3** (8.5 mg, 20 μmol) in super dehydrated DMF (350 μL) were added HBTU (1.6 mg, 4.3 μmol), Alexa Flour 488 (3 mg, 3.6 μmol), and DIPEA (5.2 mg, 40 μmol). The reaction mixture was allowed to stir for 12 hr at r.t. The product was purified with reversed–phase HPLC to give a compound **5** as an orange solid. To a stirred solution of compound **5** in THF (100 μL) and H_2O (90 μL) was added 1 M NaOH (10 μL). The reaction mixture was allowed to stir for 20 min at 50 °C. The solution was neutralised with 1 M HCl. The solvent was evaporated and the residue was dissolved in MeOH. The reaction solution was filtered and the solvent was removed by evaporation to give Gzn-Ax488 (94 μg, 0.1 μmol, 2.8%). HR-ESI MS: calcd for $C_{45}H_{40}N_6O_{13}S_2$ $[M-2H+Na]^-$ = 979.1661: obsd = 979.1660.

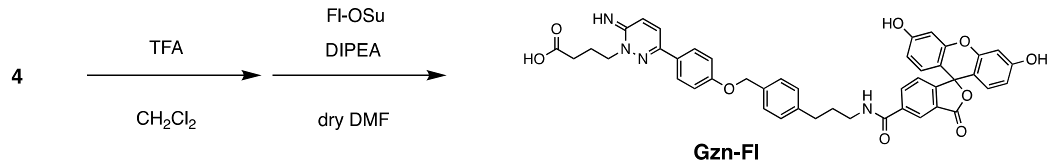

Synthesis of Gzn-Fl

4-(3-(4-((4-(3-(3',6'-dihydroxy-3-oxo-3*H*-spiro[isobenzofuran-1,9'-xanthene]-5-carboxamido)propyl)benzyl)oxy)phenyl)-6-iminopyridazin-1(6*H*)-yl)butanoic acid

To a stirred solution of compound **4** (3 mg, 5.6 μmol) in CH_2Cl_2 (1 mL) was added TFA (1 mL), and the reaction mixture was allowed to stir for 30 min at r.t. After azetoropic removal of TFA with toluene (2 mL x 2), the residue was dissolved in dry DMF (560 μL). Then, 5-carboxyfluorescein succinimide ester (Fl-OSu) (2.1 mg, 4.2 μmol, 0.75 eq.) and DIPEA (14.9 mg, 115 μmol, 21 eq.)

were added. The reaction mixture was stirred at r.t. for 0.5 h. The solution was purified by reversed-phase HPLC to yield compound Gzn-Fl (192 μg, 246 μmol, 4.4%). HR-ESI MS: calcd for $C_{45}H_{38}N_4O_9$ $[M+H]^+$ = 779.2712: obsd = 779.2713.

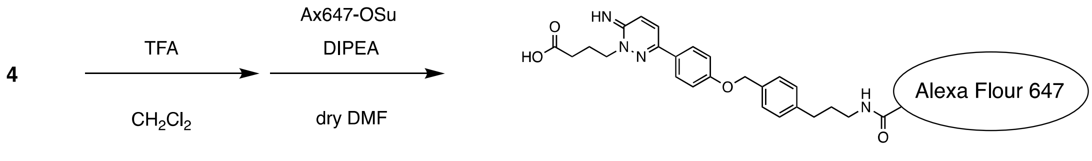

Gzn-Ax647

Synthesis of Gzn-Ax647

To a stirred solution of compound **4** (0.5 mg, 0.96 μmol) in CH_2Cl_2 (1 mL) was added TFA (1 mL), and the reaction mixture was allowed to stir for 30 min at r.t. After azetoropic removal of TFA with toluene (2 mL x 2), the residue was dissolved in dry DMF (200 μL). Then, Alexa Flour 647 succinimide ester (Ax647-OSu) (1 mg, 0.8 μmol, 0.8 eq.) and DIPEA (14.9 mg, 115 μmol, 120 eq.) were added. The reaction mixture was stirred at r.t. for 1 h. The solution was purified by reversed-phase HPLC to yield compound Gzn-Ax647 (250 μg, 0.19 μmol, 20%). HR-ESI MS: calcd for $C_{60}H_{72}N_6O_{16}S_4$ $[M–2H]^{2-}$ =629.1871: obsd = 629.1870.

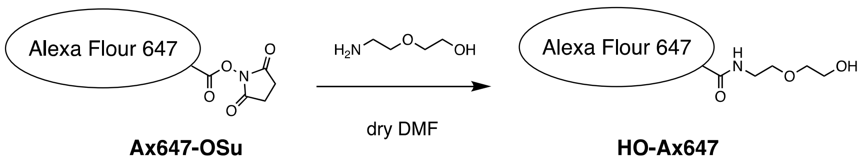

Ax647-OSu **HO-Ax647**

Synthesis of HO-Ax647

Ax647-OSu (1 mg, 1 μmol) was dissolved into 0.1 mL of super dehydrated DMF. 2-(2-Aminoethoxy)ethanol (9.5 mg, 91 μmol, 91 equiv.) was added and the reaction solution was stirred at r.t. under Ar atmosphere for 1 hr. The solution was purified by reversed-phase HPLC to yield compound HO-Ax647 (0.15 mg, 0.15 μmol, 15%). HR-ESI MS: calcd for $C_{40}H_{55}N_3NO_{15}S_4$ $[M–3H]^{3-}$ = 314.0770: obsd = 314.0768.

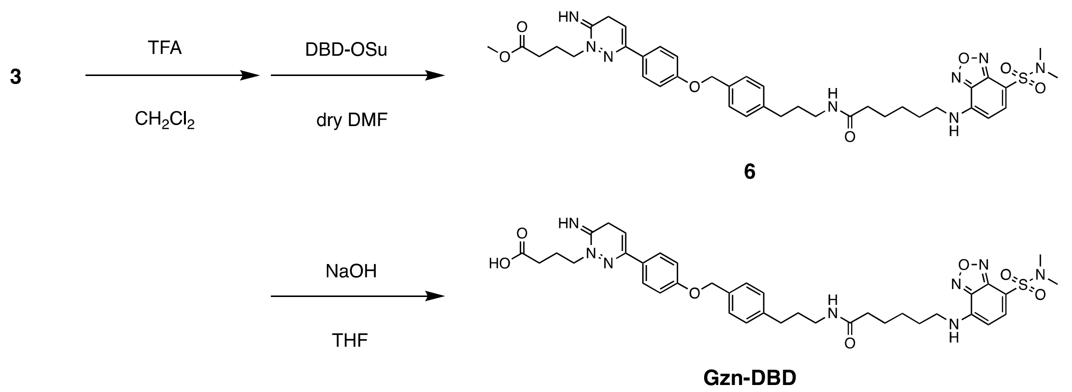

Synthesis of Gzn-DBD

4-(3-(4-((4-(3-(6-((7-(*N*,*N*-dimethylsulfamoyl)benzo[*c*][1,2,5]oxadiazol-4-yl)amino)hexanamido)propyl)benzyl)oxy)phenyl)-6-iminopyridazin-1(6*H*)-yl)butanoic acid

To a stirred solution of compound **3** (20 mg, 37 μmol) in CH_2Cl_2 (2 mL) was added TFA (1 mL), and the reaction mixture was allowed to stir for 30 min at r.t. After azetoropic removal of TFA with toluene (2 mL x 2), the residue was dissolved in dry DMF (500 μL). Then, Succinimidyl 6-[[7-(*N*,*N*-Dimethylaminosulfonyl)-2,1,3-benzoxadiazol-4-yl]amino]hexanoate (DBD-OSu) (26 mg, 57 μmol, 1.5 eq.) and DIPEA (18 mg, 138 μmol, 3.7 eq.) were added. The reaction mixture was stirred at r.t. for 12 h. The solution was purified by silica gel column chromatography ($CHCl_3$: MeOH : 28% NH_3 aq. = 10:1:0.1) to yield compound **6**. To a stirred solution of compound **6** in THF (150 μL) and H_2O (107 μL) was added 1 M NaOH (47 μL). The reaction mixture was allowed to stir for 20 min at 50 °C. The solution was neutralised with 1 M HCl. The solvent was evaporated and the residue was dissolved in MeOH. The reaction solution was filtered and the solvent was removed by evaporation to give Gzn-DBD (14.5 mg, 19.1 μmol, 51%). ^{1}H-NMR (400 MHz, CD_3OD): δ 8.26 (d, J = 7.2 Hz, 1H), 7.94 (d, 2H, J = 8.8 Hz), 7.85 (d, 1H, J = 8.4 Hz), 7.62 (d, 1H, J = 9.6 Hz), 7.37 (d, 2H, J = 8.0 Hz), 7.23 (d, 2H, J = 8.0 Hz), 7.14 (d, 2H, J = 8.4 Hz), 6.25 (d, 2H, J = 8.4 Hz), 5.15 (s, 2H), 6.88 (s, 1H), 4.44 (t, 2H, J = 7.6 Hz), 3.44 (t, 2H, J = 6.6 Hz), 3.21 (t, 2H, J = 6.6 Hz), 2.80 (s, 6H), 2.66 (t, 2H, J = 7.4 Hz), 2.40 (t, 2H, J = 6.0 Hz), 2.33 (m, 2H), 2.16 (t, 2H, J = 7.6 Hz), 1.83 (m, 2H), 1.79 (m, 2H), 1.70 (m, 2H), 1.49 (m, 2H). ^{13}C-NMR-dept (600 MHz, DMSO-d6): : δ 180.41, 176.03, 162.61, 153.84, 151.74, 147.91, 145.77, 143.20, 142.98, 141.63, 135.74, 132.32, 129.62, 129.26, 128.87, 126.75, 126.44, 116.59, 107.28, 99.40, 71.03, 57.73, 44.24, 39.99,38.18, 36.91, 33.93, 33.49, 32.10, 29.07, 27.65, 26.63, 24.03. HR-ESI MS: calcd for $C_{38}H_{46}N_8O_7S$ $[M+H]^+$ = 759.3283: obsd = 759.3283.

Supporting Reference

S1. Yamaura, K.; Kiyonaka, S.; Numata, T.; Inoue, R.; Hamachi, I. Discovery of Allosteric Modulators for $GABA_A$ Receptors by Ligand-Directed Chemistry. *Nat. Chem. Biol.* **2016**, *12*, 822–830.